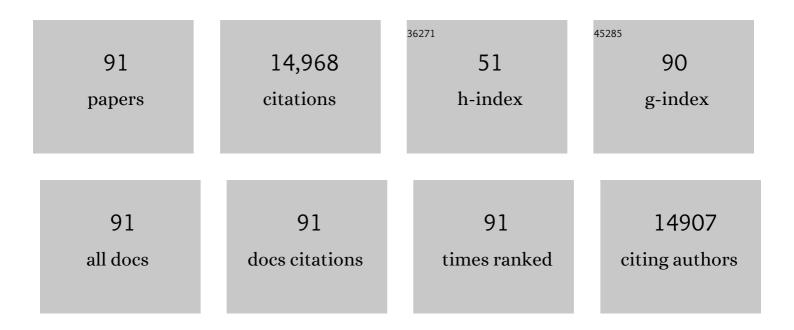
List of Publications by Year in descending order

Source: https://exaly.com/author-pdf/6622732/publications.pdf Version: 2024-02-01



YII MANC

#	Article	IF	CITATIONS
1	Two-dimensional metallic tantalum ditelluride with an intrinsic basal-plane activity for oxygen reduction: A microkinetic modeling study. Green Energy and Environment, 2022, 7, 525-532.	4.7	5
2	2D Pentagonal Pdâ€Based Janus Transition Metal Dichalcogenides for Photocatalytic Water Splitting. Physica Status Solidi - Rapid Research Letters, 2022, 16, 2100344.	1.2	17
3	Au(111)@Ti ₆ O ₁₁ heterostructure composites with enhanced synergistic effects as efficient electrocatalysts for the hydrogen evolution reaction. Nanoscale, 2022, 14, 3878-3887.	2.8	5
4	NP monolayer supported transition-metal single atoms for electrochemical water splitting: a theoretical study. Physical Chemistry Chemical Physics, 2022, 24, 10325-10333.	1.3	7
5	Pentagonal PdX2 (X = S, Se) nanosheets with X vacancies as high-performance electrocatalysts for the hydrogen evolution reaction. Physical Chemistry Chemical Physics, 2022, , .	1.3	2
6	Activity Origin of Antimony Nanosheets toward Selective Electroreduction of CO ₂ to Formic Acid. Journal of Physical Chemistry C, 2022, 126, 4015-4023.	1.5	7
7	Efficient and Selective CO ₂ Reduction to Formate on Pdâ€Doped Pb ₃ (CO ₃) ₂ (OH) ₂ : Dynamic Catalyst Reconstruction and Accelerated CO ₂ Protonation. Small, 2022, 18, e2107885.	5.2	18
8	1T′-MoTe2 monolayer: A promising two-dimensional catalyst for the electrochemical production of hydrogen peroxide. Chinese Journal of Catalysis, 2022, 43, 1520-1526.	6.9	4
9	Why heterogeneous single-atom catalysts preferentially produce CO in the electrochemical CO ₂ reduction reaction. Chemical Science, 2022, 13, 6366-6372.	3.7	35
10	Atomically dispersed Ni–Ru–P interface sites for high-efficiency pH-universal electrocatalysis of hydrogen evolution. Nano Energy, 2021, 80, 105467.	8.2	114
11	Transitionâ€Metal Carbides as Hydrogen Evolution Reduction Electrocatalysts: Synthetic Methods and Optimization Strategies. Chemistry - A European Journal, 2021, 27, 5074-5090.	1.7	41
12	Tracking structural evolution: <i>operando</i> regenerative CeOx/Bi interface structure for high-performance CO2 electroreduction. National Science Review, 2021, 8, nwaa187.	4.6	50
13	Highly Boosted Reaction Kinetics in Carbon Dioxide Electroreduction by Surfaceâ€Introduced Electronegative Dopants. Advanced Functional Materials, 2021, 31, 2008146.	7.8	88
14	Temperature-sensitive spatial distribution of defects in <mml:math xmlns:mml="http://www.w3.org/1998/Math/MathML"><mml:mrow><mml:mi>Pd</mml:mi><mml:msub><mml: flakes. Physical Review Materials, 2021, 5, .</mml: </mml:msub></mml:mrow></mml:math 	mi> &e /m	ml:mi> <mml:r< td=""></mml:r<>
15	Laserâ€Induced Annealing of Metal–Organic Frameworks on Conductive Substrates for Electrochemical Water Splitting. Advanced Functional Materials, 2021, 31, 2102648.	7.8	47
16	NiTe Monolayer: Two-Dimensional Metal with Superior Basal-Plane Activity for the Oxygen Reduction Reaction. Journal of Physical Chemistry C, 2021, 125, 19164-19170.	1.5	12
17	Polyoxometalateâ€Based Metal–Organic Framework as Molecular Sieve for Highly Selective Semiâ€Hydrogenation of Acetylene on Isolated Single Pd Atom Sites. Angewandte Chemie, 2021, 133, 22696-22702.	1.6	10
18	Polyoxometalateâ€Based Metal–Organic Framework as Molecular Sieve for Highly Selective Semiâ€Hydrogenation of Acetylene on Isolated Single Pd Atom Sites. Angewandte Chemie - International Edition, 2021, 60, 22522-22528.	7.2	112

#	Article	IF	CITATIONS
19	The tripartite role of 2D covalent organic frameworks in graphene-based organic solvent nanofiltration membranes. Matter, 2021, 4, 2953-2969.	5.0	24
20	Two Birds with One Stone: Surface Functionalization and Delamination of Multilayered Ti ₃ C ₂ T _{<i>x</i>} MXene by Grafting a Ruthenium(II) Complex to Achieve Conductivity-Enhanced Electrochemiluminescence. Analytical Chemistry, 2021, 93, 1834-1841.	3.2	39
21	Origin of the N-coordinated single-atom Ni sites in heterogeneous electrocatalysts for CO ₂ reduction reaction. Chemical Science, 2021, 12, 14065-14073.	3.7	35
22	β-PdBi2 monolayer: two-dimensional topological metal with superior catalytic activity for carbon dioxide electroreduction to formic acid. Materials Today Advances, 2020, 8, 100091.	2.5	14
23	Discovery of main group single Sb–N ₄ active sites for CO ₂ electroreduction to formate with high efficiency. Energy and Environmental Science, 2020, 13, 2856-2863.	15.6	245
24	Embedding Ultrafine Metal Oxide Nanoparticles in Monolayered Metal–Organic Framework Nanosheets Enables Efficient Electrocatalytic Oxygen Evolution. ACS Nano, 2020, 14, 1971-1981.	7.3	109
25	Design of a Singleâ€Atom Indium ^{δ+} –N ₄ Interface for Efficient Electroreduction of CO ₂ to Formate. Angewandte Chemie - International Edition, 2020, 59, 22465-22469.	7.2	232
26	Design of a Singleâ€Atom Indium δ+ –N 4 Interface for Efficient Electroreduction of CO 2 to Formate. Angewandte Chemie, 2020, 132, 22651-22655.	1.6	29
27	Tuning the Electronic Structures of Multimetal Oxide Nanoplates to Realize Favorable Adsorption Energies of Oxygenated Intermediates. ACS Nano, 2020, 14, 17640-17651.	7.3	56
28	Planar Hypercoordinate Motifs in Two-Dimensional Materials. Accounts of Chemical Research, 2020, 53, 887-895.	7.6	54
29	Highly Efficient Hydrogenation of Nitroarenes by N-Doped Carbon-Supported Cobalt Single-Atom Catalyst in Ethanol/Water Mixed Solvent. ACS Applied Materials & Interfaces, 2020, 12, 34021-34031.	4.0	56
30	Two-Dimensional GeTe: Air Stability and Photocatalytic Performance for Hydrogen Evolution. ACS Applied Materials & Interfaces, 2020, 12, 37108-37115.	4.0	12
31	Recent advancements in heterostructured interface engineering for hydrogen evolution reaction electrocatalysis. Journal of Materials Chemistry A, 2020, 8, 6926-6956.	5.2	158
32	Gadoliniumâ€Induced Valence Structure Engineering for Enhanced Oxygen Electrocatalysis. Advanced Energy Materials, 2020, 10, 1903833.	10.2	114
33	Realizing small-flake graphene oxide membranes for ultrafast size-dependent organic solvent nanofiltration. Science Advances, 2020, 6, eaaz9184.	4.7	177
34	Selective electrochemical production of hydrogen peroxide at zigzag edges of exfoliated molybdenum telluride nanoflakes. National Science Review, 2020, 7, 1360-1366.	4.6	40
35	Efficient Nitrate Synthesis via Ambient Nitrogen Oxidation with Ruâ€Đoped TiO ₂ /RuO ₂ Electrocatalysts. Advanced Materials, 2020, 32, e2002189.	11.1	125
36	<i>In situ</i> oxidation transformation of trimetallic selenide to amorphous FeCo-oxyhydroxide by self-sacrificing MoSe ₂ for efficient water oxidation. Journal of Materials Chemistry A, 2020, 8, 7925-7934.	5.2	40

#	Article	IF	CITATIONS
37	Efficient alkaline hydrogen evolution on atomically dispersed Ni–N _x Species anchored porous carbon with embedded Ni nanoparticles by accelerating water dissociation kinetics. Energy and Environmental Science, 2019, 12, 149-156.	15.6	416
38	Spin–Orbit Coupling-Dominated Catalytic Activity of Two-Dimensional Bismuth toward CO ₂ Electroreduction: Not the Thinner the Better. Journal of Physical Chemistry Letters, 2019, 10, 4663-4667.	2.1	41
39	Spin Selection Rule in Single-Site Catalysis of Molecular Oxygen Adsorption on Transition-Metal Phthalocyanines. Journal of Physical Chemistry C, 2019, 123, 28158-28167.	1.5	4
40	Self-Adjusting Activity Induced by Intrinsic Reaction Intermediate in Fe–N–C Single-Atom Catalysts. Journal of the American Chemical Society, 2019, 141, 14115-14119.	6.6	261
41	Bismuth Single Atoms Resulting from Transformation of Metal–Organic Frameworks and Their Use as Electrocatalysts for CO ₂ Reduction. Journal of the American Chemical Society, 2019, 141, 16569-16573.	6.6	501
42	Boosting Oxygen Reduction Catalysis with Fe–N ₄ Sites Decorated Porous Carbons toward Fuel Cells. ACS Catalysis, 2019, 9, 2158-2163.	5.5	297
43	Superior Oxygen Electrocatalysis on Nickel Indium Thiospinels for Rechargeable Zn–Air Batteries. , 2019, 1, 123-131.		199
44	<i>In situ</i> growth of a POMOF-derived nitride based composite on Cu foam to produce hydrogen with enhanced water dissociation kinetics. Journal of Materials Chemistry A, 2019, 7, 13559-13566.	5.2	39
45	BN Pairs Enriched Defective Carbon Nanosheets for Ammonia Synthesis with High Efficiency. Small, 2019, 15, e1805029.	5.2	164
46	Solid-Diffusion Synthesis of Single-Atom Catalysts Directly from Bulk Metal for Efficient CO2 Reduction. Joule, 2019, 3, 584-594.	11.7	277
47	Ultrathin bismuth nanosheets from in situ topotactic transformation for selective electrocatalytic CO2 reduction to formate. Nature Communications, 2018, 9, 1320.	5.8	658
48	A two-dimensional CaSi monolayer with quasi-planar pentacoordinate silicon. Nanoscale Horizons, 2018, 3, 327-334.	4.1	51
49	The germanium telluride monolayer: a two dimensional semiconductor with high carrier mobility for photocatalytic water splitting. Journal of Materials Chemistry A, 2018, 6, 4119-4125.	5.2	87
50	Porous silaphosphorene, silaarsenene and silaantimonene: a sweet marriage of Si and P/As/Sb. Journal of Materials Chemistry A, 2018, 6, 3738-3746.	5.2	14
51	Core–Shell ZIF-8@ZIF-67-Derived CoP Nanoparticle-Embedded N-Doped Carbon Nanotube Hollow Polyhedron for Efficient Overall Water Splitting. Journal of the American Chemical Society, 2018, 140, 2610-2618.	6.6	1,556
52	Ru Modulation Effects in the Synthesis of Unique Rod-like Ni@Ni ₂ P–Ru Heterostructures and Their Remarkable Electrocatalytic Hydrogen Evolution Performance. Journal of the American Chemical Society, 2018, 140, 2731-2734.	6.6	326
53	Defect Effects on TiO ₂ Nanosheets: Stabilizing Single Atomic Site Au and Promoting Catalytic Properties. Advanced Materials, 2018, 30, 1705369.	11.1	751
54	A "Signal On―Photoelectrochemical Biosensor Based on Bismuth@N,Oâ€Codopedâ€Carbon Coreâ€Shell Nanohybrids for Ultrasensitive Detection of Telomerase in HeLa Cells. Chemistry - A European Journal, 2018, 24, 3677-3682.	1.7	35

#	Article	IF	CITATIONS
55	Single Pt Atoms Confined into a Metal–Organic Framework for Efficient Photocatalysis. Advanced Materials, 2018, 30, 1705112.	11.1	599
56	Boosting hydrogen evolution <i>via</i> optimized hydrogen adsorption at the interface of CoP ₃ and Ni ₂ P. Journal of Materials Chemistry A, 2018, 6, 5560-5565.	5.2	107
57	Pd ₂ Se ₃ monolayer: a novel two-dimensional material with excellent electronic, transport, and optical properties. Journal of Materials Chemistry C, 2018, 6, 4494-4500.	2.7	36
58	Low Overpotential for Electrochemically Reducing CO ₂ to CO on Nitrogen-Doped Graphene Quantum Dots-Wrapped Single-Crystalline Gold Nanoparticles. ACS Energy Letters, 2018, 3, 946-951.	8.8	48
59	Quaternary bimetallic phosphosulphide nanosheets derived from prussian blue analogues: Origin of the ultra-high activity for oxygen evolution. Journal of Power Sources, 2018, 403, 90-96.	4.0	87
60	PtTe Monolayer: Two-Dimensional Electrocatalyst with High Basal Plane Activity toward Oxygen Reduction Reaction. Journal of the American Chemical Society, 2018, 140, 12732-12735.	6.6	95
61	Selective CO ₂ Reduction on 2D Mesoporous Bi Nanosheets. Advanced Energy Materials, 2018, 8, 1801536.	10.2	274
62	Stabilizing and Activating Metastable Nickel Nanocrystals for Highly Efficient Hydrogen Evolution Electrocatalysis. ACS Nano, 2018, 12, 11625-11631.	7.3	55
63	PdSeO ₃ Monolayer: Promising Inorganic 2D Photocatalyst for Direct Overall Water Splitting Without Using Sacrificial Reagents and Cocatalysts. Journal of the American Chemical Society, 2018, 140, 12256-12262.	6.6	216
64	Porous hexagonal boron oxide monolayer with robust wide band gap: A computational study. FlatChem, 2018, 9, 27-32.	2.8	29
65	<i>Operando</i> X-ray spectroscopic tracking of self-reconstruction for anchored nanoparticles as high-performance electrocatalysts towards oxygen evolution. Energy and Environmental Science, 2018, 11, 2945-2953.	15.6	157
66	Single Tungsten Atoms Supported on MOFâ€Derived Nâ€Doped Carbon for Robust Electrochemical Hydrogen Evolution. Advanced Materials, 2018, 30, e1800396.	11.1	427
67	Tetra-silicene: A Semiconducting Allotrope of Silicene with Negative Poisson's Ratios. Journal of Physical Chemistry C, 2017, 121, 9627-9633.	1.5	57
68	Tuning Unique Peapod‣ike Co(S <i>_x</i> Se _{1–} <i>_x</i>) ₂ Nanoparticles for Efficient Overall Water Splitting. Advanced Functional Materials, 2017, 27, 1701008.	7.8	192
69	CoV ₂ O ₆ –V ₂ O ₅ Coupled with Porous N-Doped Reduced Graphene Oxide Composite as a Highly Efficient Electrocatalyst for Oxygen Evolution. ACS Energy Letters, 2017, 2, 1327-1333.	8.8	84
70	Rational Design of Single Molybdenum Atoms Anchored on Nâ€Đoped Carbon for Effective Hydrogen Evolution Reaction. Angewandte Chemie - International Edition, 2017, 56, 16086-16090.	7.2	431
71	Rational Design of Single Molybdenum Atoms Anchored on Nâ€Doped Carbon for Effective Hydrogen Evolution Reaction. Angewandte Chemie, 2017, 129, 16302-16306.	1.6	82
72	Benzene-like N ₆ rings in a Be ₂ N ₆ monolayer: a stable 2D semiconductor with high carrier mobility. Journal of Materials Chemistry C, 2017, 5, 11515-11521.	2.7	15

#	Article	IF	CITATIONS
73	Filling the oxygen vacancies in Co ₃ O ₄ with phosphorus: an ultra-efficient electrocatalyst for overall water splitting. Energy and Environmental Science, 2017, 10, 2563-2569.	15.6	859
74	Supported Cobalt Polyphthalocyanine for High-Performance Electrocatalytic CO2 Reduction. CheM, 2017, 3, 652-664.	5.8	406
75	Effective Interlayer Engineering of Two-Dimensional VOPO ₄ Nanosheets via Controlled Organic Intercalation for Improving Alkali Ion Storage. Nano Letters, 2017, 17, 6273-6279.	4.5	102
76	Cesium Lead Halide Perovskite Quantum Dots as a Photoluminescence Probe for Metal Ions. Advanced Materials, 2017, 29, 1700150.	11.1	112
77	Two-dimensional iron-porphyrin sheet as a promising catalyst for oxygen reduction reaction: a computational study. Science Bulletin, 2017, 62, 1337-1343.	4.3	56
78	Ultrathin Layers of PdPX (X=S, Se): Two Dimensional Semiconductors for Photocatalytic Water Splitting. Chemistry - A European Journal, 2017, 23, 13612-13616.	1.7	66
79	High-index faceted CuFeS ₂ nanosheets with enhanced behavior for boosting hydrogen evolution reaction. Nanoscale, 2017, 9, 9230-9237.	2.8	70
80	Molybdenum Disulfide/Nitrogenâ€Doped Reduced Graphene Oxide Nanocomposite with Enlarged Interlayer Spacing for Electrocatalytic Hydrogen Evolution. Advanced Energy Materials, 2016, 6, 1600116.	10.2	433
81	Two-dimensional stanane: strain-tunable electronic structure, high carrier mobility, and pronounced light absorption. Physical Chemistry Chemical Physics, 2016, 18, 14638-14643.	1.3	33
82	Two-dimensional nanostructures of non-layered ternary thiospinels and their bifunctional electrocatalytic properties for oxygen reduction and evolution: the case of CuCo ₂ S ₄ nanosheets. Inorganic Chemistry Frontiers, 2016, 3, 1501-1509.	3.0	69
83	Atomic-Scale Mechanism on Nucleation and Growth of Mo ₂ C Nanoparticles Revealed by in Situ Transmission Electron Microscopy. Nano Letters, 2016, 16, 7875-7881.	4.5	28
84	Coupled molybdenum carbide and reduced graphene oxide electrocatalysts for efficient hydrogen evolution. Nature Communications, 2016, 7, 11204.	5.8	803
85	Ultrasmall and phase-pure W2C nanoparticles for efficient electrocatalytic and photoelectrochemical hydrogen evolution. Nature Communications, 2016, 7, 13216.	5.8	334
86	Semi-metallic Be5C2 monolayer global minimum with quasi-planar pentacoordinate carbons and negative Poisson's ratio. Nature Communications, 2016, 7, 11488.	5.8	247
87	Germanium monosulfide monolayer: a novel two-dimensional semiconductor with a high carrier mobility. Journal of Materials Chemistry C, 2016, 4, 2155-2159.	2.7	212
88	Two-dimensional iron-phthalocyanine (Fe-Pc) monolayer as a promising single-atom-catalyst for oxygen reduction reaction: a computational study. Nanoscale, 2015, 7, 11633-11641.	2.8	164
89	Not your familiar two dimensional transition metal disulfide: structural and electronic properties of the PdS ₂ monolayer. Journal of Materials Chemistry C, 2015, 3, 9603-9608.	2.7	135
90	Reducing Band Gap and Enhancing Carrier Mobility of Boron Nitride Nanoribbons by Conjugated π Edge States. Journal of Physical Chemistry C, 2014, 118, 25051-25056.	1.5	25

#	Article	IF	CITATIONS
91	Preserving the edge magnetism of graphene nanoribbons by iodine termination: a computational study. Theoretical Chemistry Accounts, 2014, 133, 1.	0.5	2